Bioactive Materials 18 (2022) 368–382

Contents lists available at ScienceDirect

Bioactive Materials

journal homepage: www.keaipublishing.com/en/journals/bioactive-materials

A new hemostatic agent composed of Zn^{2+}-enriched Ca^{2+} alginate activates vascular endothelial cells *in vitro* and promotes tissue repair *in vivo*

Anne-Charlotte Ponsen [a,*], Richard Proust [a], Sabrina Soave [a], Françoise Mercier-Nomé [b,c], Isabelle Garcin [d], Laurent Combettes [d], Jean-Jacques Lataillade [a,e], Georges Uzan [a]

[a] INSERM UMRS-MD 1197, Université Paris-Saclay, Institut André Lwoff, Hôpital Paul Brousse, Villejuif, France
[b] Plateforme d'Histologie Immunopathologie de Clamart (PHIC), Université Paris-Saclay, INSERM, CNRS, Institut Paris Saclay d'Innovation Thérapeutique, Châtenay-Malabry, France
[c] Université Paris-Saclay, INSERM, Inflammation, Microbiome and Immunosurveillance, Clamart, France
[d] INSERM UMRS 1174, Université Paris-Saclay, Orsay, France
[e] Centre de Transfusion Sanguine des Armées, Clamart, France

ARTICLE INFO

Keywords:
Hemostatic agent
Alginate
Surgery
Hemostasis
Endothelial cells
Tissue repair

ABSTRACT

To control capillary bleeding, surgeons may use absorbable hemostatic agents, such as Surgicel® and TachoSil®. Due to their slow resorption, their persistence *in situ* can have a negative impact on tissue repair in the resected organ. To avoid complications and obtain a hemostatic agent that promotes tissue repair, a zinc-supplemented calcium alginate compress was developed: HEMO-IONIC®. This compress is non-absorbable and is therefore removed once hemostasis has been achieved. After demonstrating the hemostatic efficacy and stability of the blood clot obtained with HEMO-IONIC, the impact of Surgicel, TachoSil, and HEMO-IONIC on cell activation and tissue repair were compared (i) *in vitro* on endothelial cells, which are essential to tissue repair, and (ii) *in vivo* in a mouse skin excision model. *In vitro*, only HEMO-IONIC maintained the phenotypic and functional properties of endothelial cells and induced their migration. In comparison, Surgicel was found to be highly cytotoxic, and TachoSil inhibited endothelial cell migration. *In vivo*, only HEMO-IONIC increased angiogenesis, the recruitment of cells essential to tissue repair (macrophages, fibroblasts, and epithelial cells), and accelerated maturation of the extracellular matrix. These results demonstrate that a zinc-supplemented calcium alginate, HEMO-IONIC, applied for 10 min at the end of surgery and then removed has a long-term positive effect on all phases of tissue repair.

1. Introduction

Achieving good hemostasis at the end of a surgical intervention, in particular by controlling oozing due to capillary bleeding, is a major concern [1,2]. To control capillary bleeding, surgeons can apply absorbable hemostatic compresses, the most commonly used of which are Surgicel® (oxidized regenerated cellulose, Johnson & Johnson) and TachoSil® (human fibrinogen and human thrombin coated onto an equine collagen sponge, Takeda) [3,4]. Surgicel and TachoSil mechanically influence hemostasis by providing a framework for platelet aggregation; TachoSil also has a biological action as it promotes the formation of fibrin. Numerous studies have demonstrated the hemostatic efficacy of these products [5–9]. Despite this recognized efficacy, post-operative complications – including tissue necrosis, hypersensitivity, allergy, stenosis, thromboembolic complications, sepsis – have been reported in several publications due to their presence *in situ* and slow resorption [10–16]. In addition, few studies have assessed the impact of hemostatic agents on tissue repair mechanisms. Indeed, as these agents remain *in situ*, and due to their slow resorption (from weeks to months) they may cause foreign body reactions and interfere with repair of the resected organ [17,18]. This may be an issue as the speed of post-surgical organ repair is known to have a direct influence on the patient's recovery [19–21]. It thus appears essential to ensure that any hemostatic agent used is not deleterious to the formation of new tissue, and preferably it should promote it.

The present study was designed to compare the impact on tissue

Peer review under responsibility of KeAi Communications Co., Ltd.
* Corresponding author. INSERM UMRS-MD 1197, Hôpital Paul Brousse, 12-14 avenue Paul Vaillant Couturier, 94807, Villejuif, France.
E-mail address: anne-charlotte.ponsen@inserm.fr (A.-C. Ponsen).

https://doi.org/10.1016/j.bioactmat.2022.01.049
Received 8 September 2021; Received in revised form 28 January 2022; Accepted 28 January 2022
Available online 12 February 2022
2452-199X/© 2022 The Authors. Publishing services by Elsevier B.V. on behalf of KeAi Communications Co. Ltd. This is an open access article under the CC BY-NC-ND license (http://creativecommons.org/licenses/by-nc-nd/4.0/).

repair of Surgicel and TachoSil to that of HEMO-IONIC®, a new non-absorbable hemostatic compress composed of Zn^{2+}-enriched Ca^{2+} alginate. The hemostatic properties of Ca^{2+} alginate are widely recognized [22–24] and its capacity to stimulate wound healing has been demonstrated by several basic research and clinical studies [22,25,26]. Upon contact with blood and exudate, calcium ions are released by the alginate, they then act as both an extracellular stimulus and an intracellular signal to activate the platelets [26,27] and cells required for tissue repair [28]. The inclusion of Zn^{2+}, another extracellular stimulus which triggers an intracellular calcium signal [29–31], should accentuate the hemostasis and healing induced by the calcium alginate [27,32,33].

Upon contact of HEMO-IONIC with blood, ion exchange takes place, switching the calcium and zinc ions with sodium ions from the blood. The calcium (coagulation factor IV) and zinc ions released ensure the formation of a lasting blood clot in the wound [26,27,34]. Simultaneously, the insoluble calcium alginate is transformed into a sodium alginate hydrogel, which is easy to remove from the clot without causing renewed trauma [26,35]. Hence, thanks to its bioactivity (ion exchange), HEMO-IONIC can be removed from the surgical site without triggering a resumption of bleeding [36]. In addition to the extensively demonstrated healing properties of Ca^{2+} alginate, the fact that the Zn^{2+}-enriched Ca^{2+} alginate is removed from the surgical site should also encourage repair of the resected organ by eliminating the risk of foreign body reactions. Such reactions have been observed with Surgicel and TachoSil, which remain *in situ* [17,18]. Indeed, Surgicel and TachoSil serve as frameworks for platelets that aggregate within them [2,8], and their withdrawal would remove the newly formed blood clot leading to a resumption of bleeding.

Endothelial cells are at the interface between blood and tissues. They are the key components of the vascular system and are involved in all phases of hemostasis and tissue repair. Their central role is recognized and has been demonstrated in regeneration of the skin [37], liver [38–40], lung [41,42], pancreas [43,44], and heart [45,46], among other tissues. During the inflammatory phase, endothelial cells regulate the transmigration of immune cells such as macrophages into tissues [47,48]. Endothelial cells also ensure the development of granulation tissue by forming new blood vessels, which transport oxygen and nutrients, in particular to fibroblasts involved in the reconstruction and maturation of the extracellular matrix [49–52].

Endothelial cells can be derived from a variety of stem and progenitor cells [53,54]. In this study, we used endothelial cells derived from human cord blood circulating endothelial progenitor cells (EPCs). EPCs give rise in culture to Endothelial Colony Forming Cells (ECFCs) which display interesting features. First, in contrast to more mature endothelial cells, which have specialized tissue specific features, ECFCs are not specialized and represent generic endothelial cells, which have been demonstrated to be able to perform neo-angiogenesis *in vivo* [55,56]. Second these cells are very active and stable in culture; they can be expanded without loss of function, thus limiting inter-experiment variability [57,58]. Third, these cells are easy to obtain.

As a preliminary experiment for this study on tissue repair, hemostatic efficacy and stability of blood clots were compared in *in vitro* and *in vivo* experiments using HEMO-IONIC, Surgicel, and TachoSil. The effect on cellular activation of Surgicel, TachoSil and HEMO-IONIC was then assessed *in vitro* on endothelial cells. Finally, the impact of the three hemostatic agents on tissue repair was assessed *in vivo* in a murine skin excision model.

2. Materials and methods

2.1. Hemostatic agents

Surgicel is a knitted compress composed of oxidized regenerated cellulose (Johnson and Johnson, Somerville, NJ, USA). TachoSil is a human fibrinogen/thrombin-coated patch of equine collagen (Takeda, Osaka, Japan). Surgicel and TachoSil are absorbable materials and according to their notices, only excess Surgicel and no portion of TachoSil should be removed. HEMO-IONIC is a non-woven calcium alginate compress enriched with zinc gluconate by spraying (Fig. 1A). Alginates are polysaccharides composed of two monomers of L-guluronic acid (G) and D-mannuronic acid (M). The proportion and distribution of these two monomers determines the physiochemical properties of alginate. Calcium alginate-based dressings with high guluronic acid levels retain their basic structure and, consequently, are non-absorbable materials that should be removed from lesions [59]. The predominantly guluronic calcium alginate fibers that make up HEMO-IONIC are obtained after extrusion of a solution of sodium alginate/cupric chlorophyllin (E141) through a die in a calcium chloride bath. The fibers produced are carded and then needle-punched to obtain calcium alginate compresses. These compresses are then enriched with zinc gluconate by spraying. HEMO-IONIC is a product in development at Laboratoires BROTHIER (Nanterre, France).

2.2. Endothelial colony Forming Cell (ECFC) isolation from human umbilical cord blood

Cord blood (CB) samples were obtained from the cord blood bank at St Louis hospital (Paris, France; ANSM authorization PPC51). Samples were collected from umbilical cords from healthy, full-term newborns, after obtaining informed consent from the mothers. CB Mononuclear cells (CBMCs) were collected following centrifugation of the cord blood on a Ficoll gradient (PAN-Biotech, Dutscher). CBMCs were then seeded at 20.10^6 cells per well in 12-well plates coated with 50 µg/mL rat tail collagen type I (Corning, Boulogne-Billancourt), and containing EGM-2-MV culture medium (Lonza, Basel, Switzerland). The coating encouraged adhesion of endothelial progenitors from among the CBMCs. Culture medium was renewed every day for 7 days, then every two days until ECFC colonies appeared. ECFCs were then cultured according to the protocol described by Chevalier et al. [60]. They were used between passage 3 and passage 5 in experiments.

2.3. Preparation of conditioned media

To avoid hypoxic effects resulting from direct application of the hemostatic agents to cell cultures, the effects of the three hemostatic agents on endothelial cells were studied using conditioned media (CM), in line with the protocol presented in standard ISO 10993–12:2012. CM were prepared in EGM-2-MV culture medium (or EBM-2 basal medium supplemented with 0.2% FBS for the chemotactic migration assay). A fragment of each hemostatic agent (1 cm^2) was incubated for 10 min in 2 mL of culture medium. CM were filtered through a 0.45-µm pore filter to remove any fibers shed by the hemostatic agents. For Neutralized Surgicel CM, pH was adjusted to pH7 by addition of 1 M NaOH.

2.4. Release of calcium and zinc ions

To determine the amounts of calcium and zinc ions released by HEMO-IONIC upon exchange with the sodium ions in the solution, the Ca^{2+} and Zn^{2+} concentrations were measured in the solution by high-frequency-induced atomic emission plasma spectroscopy, according to standard ISO 11885:2007 (Flandres-Analyses, Cappelle la Grande, France). Ion concentrations were measured in EGM-2-MV medium at 0 min, 2 min, 5 min, 10 min, 30 min, 24 h and 48 h after adding HEMO-IONIC (1 cm^2/2 mL), or in control medium.

2.5. Ca^{2+} signal in ECFCs

Cytoplasmic Ca^{2+} concentrations were monitored in ECFCs using FURA-2-AM, a fluorescent indicator measuring intracellular calcium. ECFCs were seeded on glass coverslips at a density of 10.10^3 cells/cm^2 in EGM-2-MV. After 48 h, coverslips were placed in the imaging medium (NaCl 115.5 mM; KCL 5.6 mM; $MgCl_2$ 1.2 mM; NaH_2PO_4 1.2 mM;

A

Hemostatic agent	Surgicel	TachoSil	HEMO-IONIC
	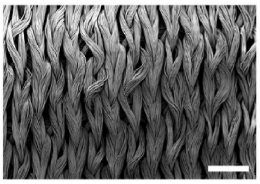	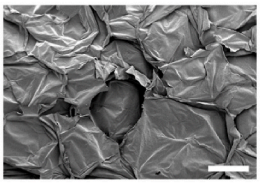	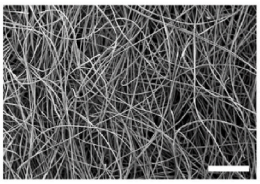
Composition	Absorbable oxidized regenerated cellulose fibers 100%	Absorbable equine collagen matrix coated with human fibrinogen and human thrombin on its active side (colored in yellow by riboflavin)	Non-absorbable calcium alginate fibers (99%) colored in green by adding chlorophyllin and enriched in zinc ions
Size	2.5 x 7.5 cm	9.5 x 4.8 cm	10 x 20 cm
Density (mg/cm²)	18.4 ±0.4 (n=7)	16 ±0.9 (n=7)	42.2 ±1.8 (n=7)
Presentation	Knitted compress	Sponge	Needled non-woven compress
Sterilization	γ-irradiation	γ-irradiation	β-irradiation
Mechanism of action	Framework for platelet aggregation [2]	Framework for platelet aggregation Thrombin and fibrinogen supply (fibrin clot formation) [8]	Ion exchange: ▪ Calcium and zinc release (platelet activation and fibrin clot formation) ▪ Gel formation [26]

B

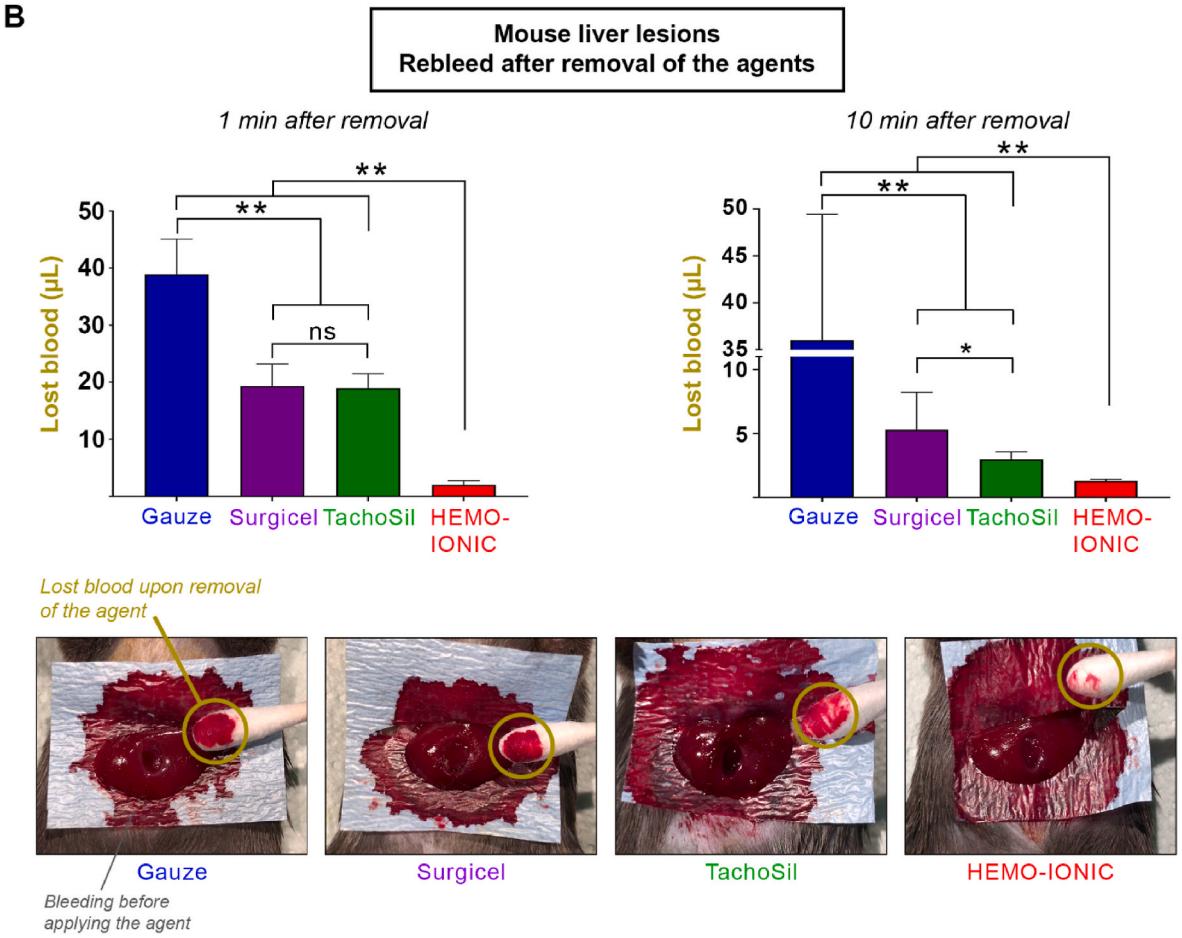

Fig. 1. HEMO-IONIC is an efficient hemostatic agent that can be removed once hemostasis has been achieved
(A) Main physical characteristics of the hemostatic agents, Surgicel, TachoSil and HEMO-IONIC. Pictures are Scanning Electron microscopy images of the three agents. Scale bar = 1 mm. (B) Evaluation of re-bleeding from mouse liver lesions following removal of gauze or hemostatic agents based on quantification of the volume of blood lost 1 min (left) and 10 min (right) after removal (n = 6, Mann-Whitney test, *p < 0.05, **p < 0.01). Pictures showing rebleeding (absorbed by the cotton swab) after removal of each dressing.

$NaHCO_3$ 5 M; $CaCl_2$ 1.8 mM; HEPES 20 M; Glucose 5.5 mM) with 3 μM FURA-2-AM molecular probe and incubated for 30 min at room temperature in the dark. After washing, coverslips were placed under permanent flux in contact with EGM-2-MV which was switched to HEMO-IONIC CM. The maximal intracytoplasmic Ca^{2+} signal was measured by exposing cells to ionomycin 2 μM (Ca^{2+} ionophore), and the minimum by incubation with 20 mM EGTA (Ca^{2+} chelator). The fluorescence intensity (F) of the FURA-2-AM probe was measured at two excitation wavelengths (340 nm and 380 nm) every 3 s using an ultra-sensitive EM-CDD camera (Hamamatsu). For each cell analyzed at each time, the fluorescence ratio (R) F340/F380 was calculated and used to determine the cytoplasmic Ca^{2+} concentration, according to the following equation [61]:

$$\left[Ca^{2+}\right]_c = \frac{R - R_{min}}{R_{max} - R} x K_d x \beta$$

Where:

$[Ca^{2+}]_c$ = concentration of cytoplasmic calcium ions
$R = F_{340nm}/F_{380nm}$
R_{min} = R in conditions where $[Ca^{2+}]_c$ is minimal (with EGTA)
R_{max} = R in conditions where $[Ca^{2+}]_c$ is maximal (with Ionomycin)
K_d = dissociation constant between Ca^{2+} and the FURA-2-AM probe = 225 nM
$\beta = F_{380nm}$ in conditions where $[Ca^{2+}]_c$ is minimal/F_{380nm} in conditions where $[Ca^{2+}]_c$ is maximal

2.6. Cell viability

To assess the effect of hemostatic agents on ECFC viability, cells were incubated for 45 min in Control EGM-2-MV medium, and Surgicel, TachoSil and HEMO-IONIC CM. To determine mortality levels, ECFCs were stained with Annexin V/Propidium Iodide (PI) (MBL International Corporation, Clinisciences, France). The numbers of dead cells (Annexin V and PI positive) and live cells (Annexin V and PI negative) were quantified using an Accuri C6 flow-cytometer (BD Biosciences).

2.7. ECFC phenotyping

To assess the presence of endothelial markers following exposure to the CM for the three hemostatic agents, fluorescent antibodies specific for known markers (and their isotype controls - Beckman Coulter) were used to label ECFCs for 30 min at 4 °C: anti-CD31-FITC (clone WM59, BD Biosciences), anti-CD144-PE (clone 55-7H1, Beckman Coulter, Villepinte, France), and anti-CD309-APC (clone 89106, R&D Systems, Lille, France). The fluorescence intensity of antibody-labelled ECFCs was detected and analyzed on an Accuri C6 flow-cytometer (BD Biosciences).

2.8. ECFC response to inflammatory conditions

ECFCs were cultured for 48 h in contact with control medium or CM prepared with the three hemostatic agents. A pro-inflammatory environment was induced by adding 10 ng/mL TNF-α (Bio-techne, Lille, France). After 16 h, ICAM-1 and VCAM-1 expression on the ECFC surface was measured by labelling with fluorescent anti-ICAM-1-FITC (1:50, Ozyme, Saint Quentin en Yvelines, France) and anti-VCAM-1-PE (1:20, Ozyme) antibodies, along with their isotype controls (Beckman Coulter). Cells and antibodies were incubated for 30 min at 4 °C. Data were acquired and analyzed on an Accuri C6 flow-cytometer (BD Biosciences).

2.9. Proliferation test

ECFCs were seeded overnight at 5.10^3 cells/cm^2, in EGM-2-MV medium. Cells were incubated for 15 min in PBS with 0.5 μM of the cell-permeable fluorescent dye carboxyfluorescein diacetate succinimidyl ester (CFSE) (Vybrant® CFDA SE Cell Tracer Kit – ref. V12883, Invitrogen – Thermo Fisher Scientific). ECFCs were then further cultured for 48 h, 72 h or 96 h in contact with control medium or CM prepared with the three hemostatic agents. The fluorescence intensity (I) in the ECFCs, which decreases as they divide, was recorded using an Accuri C6 flow-cytometer (BD Biosciences). The average number of cell divisions $\overline{m}$ was calculated using the following formula:

$$\overline{m} = \frac{\ln\left(\frac{I_{t0}}{I_t}\right)}{ln2}$$

I_{t0} = fluorescence intensity at time = 0
I_t = fluorescence intensity at time t (48 h, 72 h or 96 h)

2.10. Metabolic activity test

Metabolic activity was quantified by measuring the activity of mitochondrial enzymes present in ECFCs, based on degradation of MTS (3-(4,5-dimethylthiazol-2-yl)-5-(3-carboxymethoxyphenyl)-2-(4-sulfophenyl)-2H-tetrazolium salt; Promega, Charbonnières-les-Bains, France). The resulting colored formazan derivative is excreted into the culture medium.

ECFCs were seeded at 5.10^3 cells/cm^2 in 96-well plates and cultured in control medium or CM prepared with the three hemostatic agents. After 0 h, 48 h, 72 h and 96 h, culture medium was replaced by the MTS solution (170 μL RPMI-1640 + FBS 10%, 30 μL MTS per well) and cells were incubated for 2 h at 37 °C. The formazan-containing solutions were harvested, ECFCs were washed, and fresh control medium or CM was added until the next time-point. The harvested formazan-containing solution was analyzed by spectrophotometry at 490 nm (Multiskan Ex, Thermo Fisher Scientific, Villebon sur Yvette, France). A reference absorbance measurement at 630 nm was subtracted from the 490-nm values to eliminate background.

2.11. Chemotactic migration assay

Directed migration of ECFCs was assessed in 24-well plates using Boyden chambers consisting of two superposed compartments separated by a polycarbonate membrane with 8-μm pores (BD Biosciences). Membranes were coated overnight with 20 μg/mL fibronectin (Sigma) at RT to facilitate ECFC adhesion, and rehydrated with EBM-2 supplemented with 0.2% FBS. ECFCs (2.10^5 cells) were seeded in each of the upper compartments, suspended in EBM-2 supplemented with 0.2% FBS (Control medium).

Control medium and the three CM for the hemostatic agents were added to the lower compartments. Media were supplemented with 50 ng/mL VEGF (Miltenyi, Paris, France), a strong chemo-attractant for endothelial cells, and 50 μM Verapamil, a specific calcium antagonist, where indicated. ECFC migration through the membrane was allowed to proceed for 5 h at 37 °C. Cells were then fixed for 10 min in 4% Paraformaldehyde (PFA) and stained using Blue RAL 555 (RAL Diagnostics, MCL, Nemours, France). Cells that had not migrated were removed from the upper part of the membrane with a cotton swab. Membranes were mounted on slides under coverslips in 50% Glycergel® (Agilent Technologies, Les Ulis, France) and observed under a NIKON microscope. Each condition was analyzed in triplicate and 3 images/membrane were recorded. The number of cells on each image was quantified using ImageJ software (NIH).

2.12. Total ECFC lysate

ECFCs were seeded in 6-well culture plates and grown in EGM-2-MV to about 90% confluence. After washing with 1X PBS, cells were incubated in EBM-2 supplemented with 0.2% FBS overnight. ECFCs were then cultured in EBM-2 supplemented with 0.2% FBS, EBM-2

supplemented with 0.2% FBS + VEGF (50 ng/ml) or HÉMO-IONIC CM for 10 or 30 min at 37 °C. Cells were lysed at 4 °C in lysis buffer (1% Triton X-100, 20 mM Tris-HCL, 137 mM NaCl, 2 mM EDTA, 10% glycerol, 1 mM orthovanadate, 25 mM β-glycerophosphate, 2 mM Sodium pyrophosphate, 1 mM PMSF, and a complete protease inhibitor cocktail (Roche Diagnostics, Meylan, France), pH 7.4). Lysates were clarified by centrifugation (14,000×*g* for 15 min at 4 °C).

2.13. Western blot analysis

Proteins were quantified by Micro-BCA Protein Assay Kit (Thermo Fisher Scientific, Illkirch, France). Equivalent aliquots of protein (30 μg) were mixed with Laemmli buffer 2X containing 50 mM Dithiothreitol before loading and migration on SDS-polyacrylamide gels. Proteins were transferred onto a polyvinylidene difluoride membrane in an electrophoretic transfer cell system (iBLOT2, Thermo Fisher Scientific, Illkirch, France) for 4 min. Membranes were immediately blocked for 1 h with 3% BSA in TBS-T (TBS/0.2% Tween 20). Blots were subsequently probed with antibody against Phospho-p44/42 MAPK (Erk1/2) (Thr202/Tyr204) (Cell Signaling, 1/1000) or hFAB™ Rhodamine Anti-GAPDH antibody (Bio-Rad, 1/8000) for 90 min at room temperature, or with antibody against p44/42 MAPK (Erk1/2) (L34F12) (Cell Signaling, 1/1000) overnight at 4 °C. For the unlabeled antibodies, appropriate DyLight 700- and 800-conjugated secondary antibodies were used, respectively (Bio-Rad, 1/5000). Membranes were washed and antibody labeling was detected using the ChemiDoc MP Imaging System (Bio-Rad).

2.14. Animals

All experimental procedures were performed in accordance with the European Community Council Directive (2010/63/UE) for the care and use of laboratory animals. Procedures on mice were authorized by the French ministry for education, higher education and research after approval by the National Committee for Ethics in Animal Experimentation (CEEA N°26; projects 2015102910287890_v2 and 2016052316207908_v2). The procedure on pigs was ethically evaluated by the Ethics Committee on Animal Experiments n°055 and received a favorable opinion from the Ministry of Higher Education, Research and Innovation (project n°2021030517174457).

2.15. Liver lesion model

For each hemostatic agent (Surgicel, TachoSil, HEMO-IONIC) and the Control gauze, 6 male mice (8-week-old C57BL/6Rj) were anesthetized with isoflurane by inhalation. After subcutaneous administration of a painkiller (Buprenorphine 0.05 mg/kg), the skin on the mouse's belly was shaved and cleaned with EtOH 70% and Betadine® before making an abdominal skin excision. The left lobe of the liver was then injured using a 4-mm diameter biopsy punch, and the four products (control Gauze, HEMO-IONIC, Surgicel, TachoSil) were applied to the bleeding lesion. After 10 min, when hemostasis was achieved in all conditions, Gauze or hemostatic agents were removed and any rebleeding was recorded and quantified using a cotton swab to absorb the blood for 1 min. Ten minutes after removal of the hemostatic agents, a fresh cotton swab was used to evaluate rebleeding. The blood-soaked cotton swabs were incubated in 500 μl water overnight at 4 °C, and the amount of blood lost was quantified at 405 nm by spectrophotometry (Multiskan Ex, Thermo Fisher Scientific, Villebon sur Yvette, France).

2.16. Skin excision model

For each hemostatic agent (Surgicel, TachoSil, HEMO-IONIC) and the Control gauze, 12 male mice (8-week-old C57BL/6Rj) were anesthetized with isoflurane by inhalation. After subcutaneous administration of a painkiller (Buprenorphine 0.05 mg/kg), the skin on the mouse's back was shaved and cleaned with Betadine® and a 1-cm^2 circular skin excision was made in the middle of the back. In mice, lesions are mainly (80%) filled by contraction rather than by the formation of granulation tissue [62,63]. To remain close to the human process of lesion repair, which mainly involves the formation of granulation tissue [64,65], a device to limit contraction, specially designed for this study, and patented (n°FR1654097), was attached to the edges of the lesion. After cleaning the wounds with NaCl 0.9%, the four products were applied to the lesions. Gauze and HEMO-IONIC were removed after 10 min. In line with how they are used as absorbable hemostatic agents during surgery (left in place on the resected organ), TachoSil and Surgicel were left *in situ* on the lesion until the tissue was sampled. After surgery, mice were maintained in individual cages for 7 days, 14 days, or 2 months, at which time points they were sacrificed, and samples collected (4 mice sacrificed at each time-point for each product, i.e., 48 mice). Skin samples were fixed with 4% PFA, embedded in paraffin and cut into 3-μm sections.

2.17. Histology and immunohistochemistry analysis

After Heat-Induced Epitope Retrieval (HIER) with citrate buffer at pH6, immunofluorescence staining was performed on paraffin sections using primary antibodies: F4/80 (clone Cl:A3-1, AbD Serotec, 1/100), Vimentin (clone D21H3, Ozyme, 1/100) and Ki67 (clone SP6, Abcam, 1/50) followed by staining with appropriate Alexa Fluor™ 594-labelled secondary antibodies (Invitrogen, Thermo Fisher Scientific, 1/1000). Nuclei were stained with Hoechst 33342 (Invitrogen, 1/500). After aqueous mounting (PermaFluor, ThermoFisher Scientific), slides were scanned on a NanoZoomer 2.0-RS digital slide scanner (Hamamatsu, Japan). Images were digitally captured from the scanned slides using NDP.view2 software (Hamamatsu, Japan). Three sections for each sample were quantified and analyzed using ImageJ software (NIH). The fluorescence intensity, proportional to the number of labelled cells in the lesion, was measured as the sum of the pixel intensities relative to the area of the lesion (F4/80 and Vimentin_Day 7) or the area of the epithelium (Ki67_Day 14).

The number of blood vessels present within the lesions was quantified after Hematoxylin-Eosin-Safran (HES) staining of tissue sections collected at 7 days, using NDP.view software (Hamamatsu).

To assess maturation of the extracellular matrix, tissue sections harvested at 2 months were stained with picrosirius red (Abcam). The levels of collagen I and collagen III on the neoformed tissue area were analyzed on images recorded under polarized light using ImageJ software (NIH). Collagen I/III ratios were calculated, with a higher ratio reflecting more mature matrices.

3. Results

3.1. Hemostatic efficacy of HEMO-IONIC compared to Surgicel and TachoSil

The hemostatic potential of HEMO-IONIC was assessed *in vitro* in a whole-blood coagulation assay and *in vivo* by monitoring the hemostasis of pig liver lesions. The results obtained demonstrated that HEMO-IONIC is at least as effective as Surgicel and TachoSil when it comes to achieving hemostasis (Figs. S1A and S1B).

To further elucidate the molecular mechanisms involved in the cellular component of hemostasis, the impact of HEMO-IONIC on secretion of endothelin-1 (ET-1, a potent vasoconstrictor) and on expression of Tissue Factor (TF, the initiator of the extrinsic pathway) by endothelial cells were analyzed. ET-1 and TF were both significantly increased in endothelial cells following contact with HEMO-IONIC CM (Figs. S1C and S1D).

Finally, the benefit of adding Zn^{2+} to the calcium alginate dressing was assessed *in vitro* using plasma from patients treated with Heparin. Exposure to HEMO-IONIC significantly decreased the coagulation time

compared to a Zn^{2+}-free calcium alginate dressing (Fig. S1E).

3.2. Hemostasis stability after hemostatic agent removal

The stability of the newly-formed clot upon removal of the hemostatic agents was assessed on mouse liver lesions. Gauze, Surgicel and TachoSil were visibly stuck to the wounds when attempting their removal. In contrast, HEMO-IONIC was readily removed in one piece without observable adhesion (**Videos M1-M4**). Wounds started to bleed again following removal of Gauze, Surgicel and TachoSil, whereas hemostasis appeared stable following removal of HEMO-IONIC (**Videos M1-M4**). Blood loss was quantified 1 min and 10 min after removal of the hemostatic agents (Fig. 1B). The volume of lost blood was significantly reduced with Surgicel and Tachosil compared to Gauze. The volume of blood lost post-dressing-removal was close to zero with HEMO-IONIC, and was significantly lower than the volume of blood lost following removal of Gauze, Surgicel or TachoSil (Fig. 1B). These results demonstrate that HEMO-IONIC is easy to remove and that the newly formed clot is preserved upon removal. In comparison, the absorbable hemostatic agents Surgicel and TachoSil were more difficult to remove, and their removal led to renewed bleeding.

Supplementary video related to this article can be found at https://doi.org/10.1016/j.bioactmat.2022.01.049

3.3. Release of calcium and zinc ions from HEMO-IONIC

The bioactivity of HEMO-IONIC relies on exchange of its calcium and zinc ions with sodium ions present in the blood/exudate or in cell culture media. The basal Ca^{2+} concentration in the control medium was 1.86 mM. Upon incubation with HEMO-IONIC, this concentration increased progressively over time: very rapidly up to 2 min, then more moderately until 30 min ($[Ca^{2+}]_{t=2\ min}$ = 3.66 mM; $[Ca^{2+}]_{t=30\ min}$ = 4.33 mM). The Ca^{2+} concentration reached a plateau at 48 h ($[Ca^{2+}]_{t=48h}$ = 4.91 mM) (Fig. 2A).

The Zn^{2+} concentration in the medium also increased upon incubation with HEMO-IONIC, from 2.37 μM in the control medium to 23.88 μM at 2 min. The concentration stabilized after this time (Fig. 2B).

These results show that the HEMO-IONIC compress rapidly releases its calcium and zinc ions when placed in contact with a medium containing sodium ions.

3.4. Ca^{2+} signaling in ECFCs activated by HEMO-IONIC

Both Ca^{2+} and Zn^{2+} are extracellular activators capable of inducing an intracellular calcium signal [29–31,66]. The effect of the release of calcium and zinc ions from HEMO-IONIC on the activation of ECFCs was assessed based on intracellular calcium signaling.

The basal F340/F380 ratio was recorded in EGM-2-MV medium. When cells were exposed to HEMO-IONIC CM, this ratio increased. The maximal ratio was measured following the addition of ionomycin, and the ratio was subsequently returned to basal levels by the addition of EGTA (Fig. 2C).

The basal cytoplasmic Ca^{2+} concentration in ECFCs was 75.7 nM (in EGM-2-MV medium). Upon exposure to HEMO-IONIC CM, this concentration increased significantly to 859.6 nM ($p < 0.0001$) (Fig. 2D).

According to the literature [66], a cytoplasmic Ca^{2+} concentration of 500–1000 nM is sufficient to induce cell activation. Thus, during exchange of its calcium and zinc ions for sodium ions in the surrounding solution, HEMO-IONIC releases sufficient levels of ions to induce calcium signaling and cell activation.

3.5. Effect of the hemostatic agents on ECFC viability and maintenance of their endothelial phenotype

ECFC viability was 91.7% following contact with control medium, 90.2% upon exposure to TachoSil CM, and 91.5% upon exposure to HEMO-IONIC CM. With Surgicel CM, only 4.8% of cells remained viable (Fig. 3A). This drastic effect of Surgicel CM could be explained by its acidic pH (pH = 5), which is incompatible with cell viability. To allow us to perform further *in vitro* experiments with Surgicel, the pH of its CM was raised to 7 (Neutralized Surgicel CM). With Neutralized Surgicel CM, cell viability was 89.8% (Fig. 3A).

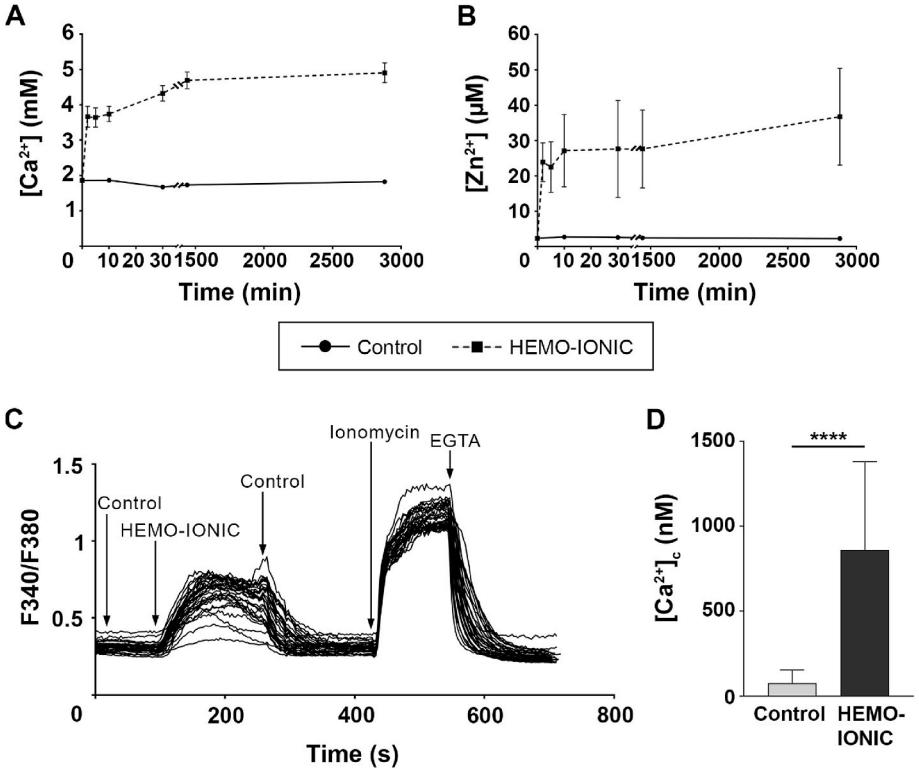

Fig. 2. HEMO-IONIC is a bioactive hemostatic agent activating calcium signaling in ECFCs
(A, B) Calcium ion concentration (A) and zinc ion concentration (B) in the medium over time after addition of HEMO-IONIC (dashed lines) and in the Control medium without HEMO-IONIC (continuous lines). (C) Evolution of the F340/F380 fluorescence ratio for the FURA-2-AM calcium probe upon contact with the Control and HEMO-IONIC-conditioned media, and following supplementation with ionomycin or EGTA (arrows indicate medium change). (D) Cytoplasmic calcium concentrations $[Ca^{2+}]c$ in ECFCs following contact with Control or HEMO-IONIC-conditioned media (mean ± SD, n = 106, Mann-Whitney test, ****$p < 0.0001$).

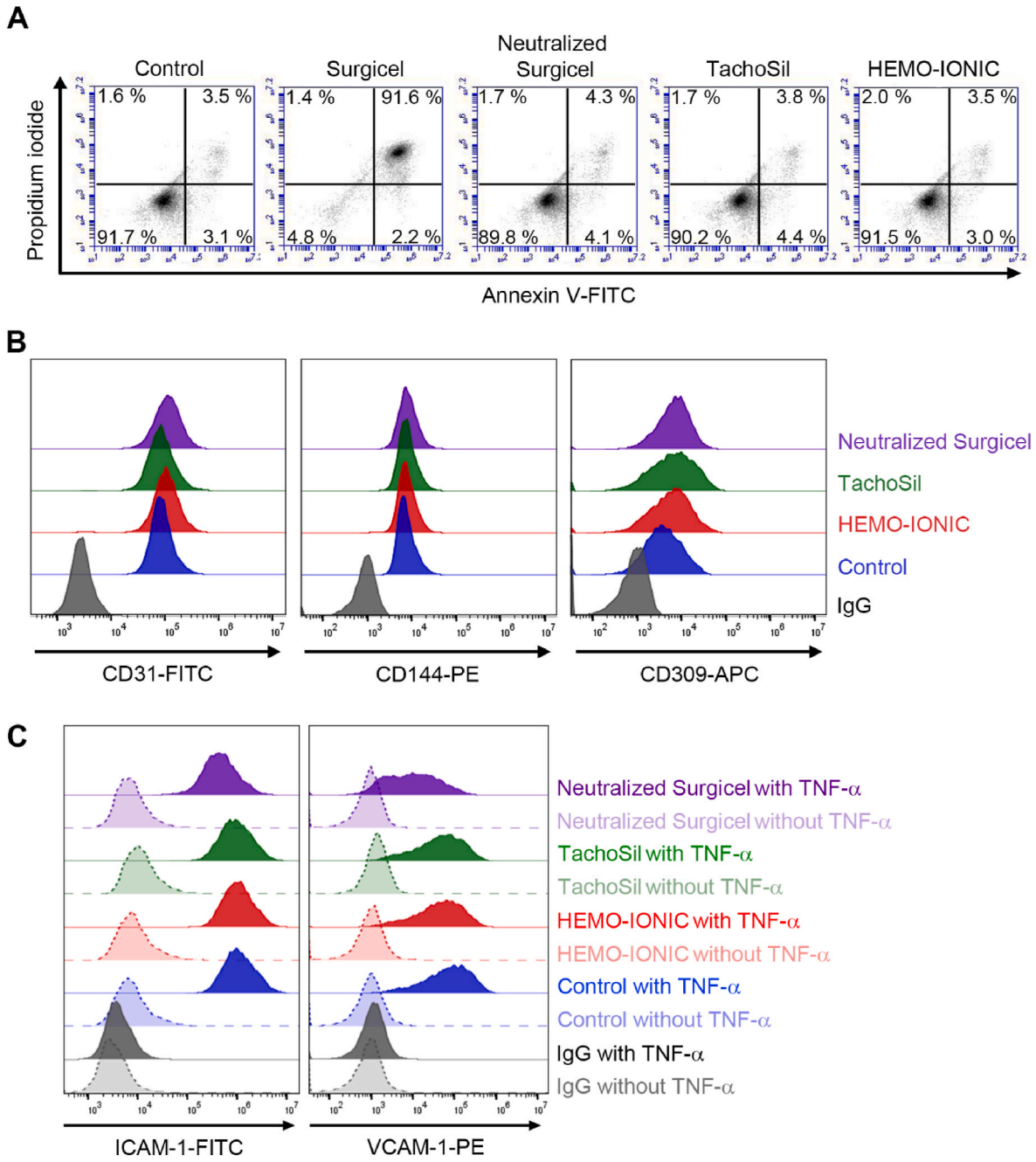

Fig. 3. ECFC characteristics are retained following contact with TachoSil and HEMO-IONIC conditioned media and with surgicel CM if neutralized
(**A**) Flow cytometry analysis of cell viability for ECFCs grown in contact with Control medium or conditioned media for the three hemostatic agents. Live cells are Annexin V- and Propidium Iodide-negative. (**B**) Flow cytometry analysis to detect endothelial markers CD31, CD144 and CD309 on the surface of ECFCs grown in Control medium or conditioned media for the three hemostatic agents. (**C**) Flow cytometry analysis in normal (without TNF-α) or pro-inflammatory (with TNF-α) conditions, to detect adhesion molecules ICAM-1 and VCAM-1 on the surface of ECFCs grown in Control medium or conditioned media for the three hemostatic agents. IgG: isotype controls.

The endothelial phenotype of ECFCs was verified based on the presence of endothelial-lineage surface markers (CD31, CD144, and CD309). Upon contact with Neutralized Surgicel, TachoSil, and HEMO-IONIC CM, ECFCs expressed the main endothelial markers at similar levels to those measured for Control cells (Fig. 3B). Thus, exposure to the three hemostatic agents maintained the endothelial phenotype.

3.6. Effect of the hemostatic agents on ECFC response to inflammatory conditions

In the inflammatory phase, endothelial cells express adhesion molecules on their surface, such as ICAM-1 and VCAM-1. These molecules allow immunological cells to tether to the endothelial surface and transmigrate across the vascular wall [48]. In non-inflammatory conditions (without TNF-α), no ICAM-1 or VCAM-1 expression was detected on the surface of ECFCs, regardless of the medium used. In pro-inflammatory conditions (with TNF-α), ECFCs expressed ICAM-1 and VCAM-1 following contact with the Control medium and CM prepared with the three hemostatic agents. With the Neutralized Surgicel CM, the molecules were expressed at lower levels than in the other conditions (Fig. 3C).

Based on these results, we can conclude that CM prepared with

Neutralized Surgicel, TachoSil and HEMO-IONIC preserve the ECFCs' response to inflammatory conditions.

3.7. Effect of the hemostatic agents on proliferation and metabolic activity in ECFCs

From 48 h, the number of cell divisions was strongly reduced for cells incubated in Neutralized Surgicel CM relative to the Control, with only 2 divisions recorded at 96 h ($p < 0.0001$). With TachoSil and HEMO-IONIC CM, the number of cell divisions was identical to the number recorded for the Control medium, with an average of 7 divisions recorded at 96 h (Fig. 4A). These results show that, even after neutralization, Surgicel inhibits ECFC proliferation, whereas TachoSil and HEMO-IONIC preserve the cells' capacity to divide.

Metabolic activity increased in a linear fashion over time in the Control medium (Fig. 4B). With Neutralized Surgicel CM, no metabolic

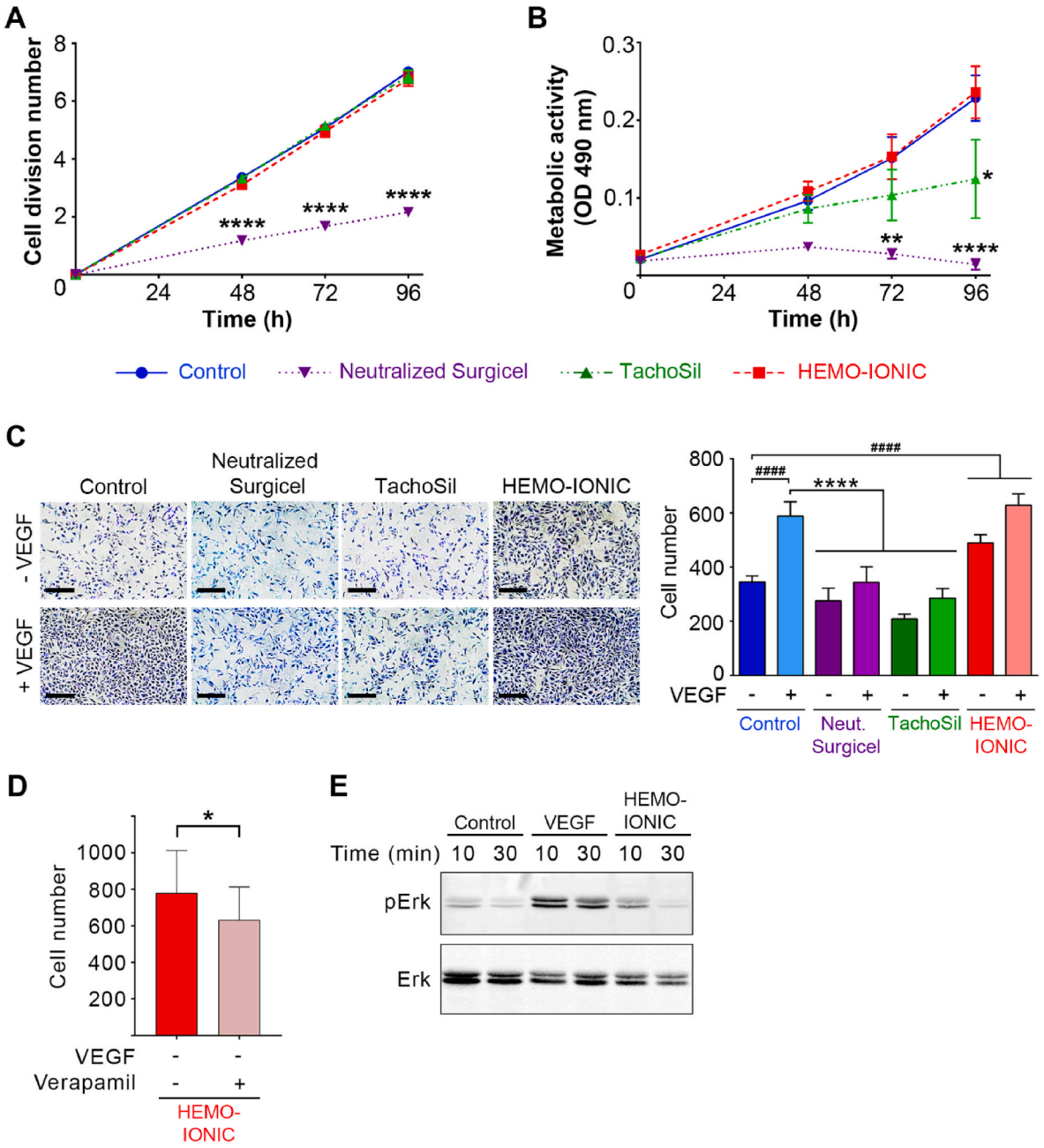

Fig. 4. Among the hemostatics tested, only HEMO-IONIC preserves proliferation and metabolic activity in ECFCs and stimulates their migration
Changes over time for ECFC cultures grown in Control medium or media conditioned with the three hemostatic agents: (A) Mean number of cell divisions measured for CFSE-labelled ECFCs (mean ± SD, n = 3, Two-way ANOVA, ****$p < 0.0001$). (B) Metabolic activity measured for ECFCs based on reduction of MTS (mean ± SD, n = 3, Two-way ANOVA, *$p < 0.05$; **$p < 0.01$; ****$p < 0.0001$). (C) Representative images and quantification of the number of ECFCs migrating across the membrane in the Boyden chamber towards the Control medium or the conditioned media for the three hemostatic agents, in the absence or presence of VEGF (mean ± SD, n = 12, Mann-Whitney test, ####$p < 0.0001$ vs Control -VEGF and ****$p < 0.0001$ vs Control + VEGF). (D) Quantification of the number of ECFCs migrating across the membrane in the Boyden chamber towards HEMO-IONIC conditioned media in the absence of VEGF and in the presence or absence of the Ca^{2+} antagonist Verapamil (mean ± SD, n = 3, Mann-Whitney test, *$p < 0.05$). (E) Representative Western Blot of pERK and total ERK on lysates of ECFCs incubated with medium alone (Control), medium containing VEGF or HEMO-IONIC CM showing an increase of pERK upon incubation with VEGF (at 10 min and 30 min) and with HEMO-IONIC (at 10 min).

activity was observed ($DO_{Neutralized\ Surgicel} = 0.03$ and 0.01 at 72 h and 96 h, respectively, $p < 0.0001$ relative to Control). In the presence of TachoSil, metabolic activity progressively decreased relative to the Control medium with a significant difference at 96 h ($DO_{TachoSil\ t=96h} = 0.12$; $p < 0.01$; Fig. 4B). In the presence of HEMO-IONIC, the metabolic activity of ECFCs increased with similar kinetics to those recorded for the Control medium until 96 h ($DO_{Control\ t=96h} = 0.23$ vs $DO_{HEMO\text{-}IONIC\ t=96h} = 0.24$). These results indicate that Surgicel and TachoSil reduce the metabolic activity of ECFCs at 96 h, and that only HEMO-IONIC fully preserves metabolic activity in ECFCs.

3.8. Effect of the hemostatic agents on directed migration of ECFCs

Relative to the negative Control without VEGF, significantly more ECFCs migrated in the positive Control with VEGF condition ($n_{Control\ -VEGF} = 345$ cells *vs* $n_{Control\ +VEGF} = 588$ cells; $p < 0.0001$; Fig. 4C). With Neutralized Surgicel and TachoSil, with or without VEGF, the numbers of cells migrating were similar to numbers for the Control without VEGF ($n_{Neutralized\ Surgicel\ -VEGF} = 275$ cells, $n_{Neutralized\ Surgicel\ +VEGF} = 343$ cells, $n_{TachoSil\ -VEGF} = 209$ cells, $n_{TachoSil\ +VEGF} = 285$ cells; $p < 0.0001$ vs $n_{Control\ +VEGF}$). In contrast, even in the absence of VEGF, HEMO-IONIC significantly increased ECFC migration relative to the Control without VEGF ($n_{HEMO\text{-}IONIC\ -VEGF} = 490$ cells, $p < 0.0001$). This VEGF-independent migration was significantly decreased in the presence of Verapamil, a specific calcium uptake antagonist ($p < 0.05$; Fig. 4D). In the presence of VEGF, HEMO-IONIC was associated with a further increase in migration, in similar proportions to that observed with VEGF-containing Control medium ($n_{HEMO\text{-}IONIC\ +\ VEGF} = 628$ cells; Fig. 4C).

These results demonstrate that, without VEGF, Neutralized Surgicel and TachoSil allow migration to a similar extent to the Control medium without VEGF, whereas HEMO-IONIC CM has a strong chemo-attractant effect, leading to significantly increased cell migration. Neutralized Surgicel CM and TachoSil CM both inhibited the chemo-attractant effect of VEGF (with cells migrating no more than in the Control without VEGF). In contrast, with HEMO-IONIC CM, ECFC migration was increased by the addition of VEGF, reaching the same level as in the Control medium with VEGF. These results show that HEMO-IONIC not only preserves the effect of VEGF but can induce cell migration even in its absence. Furthermore, the migration observed with HEMO-IONIC without VEGF was reduced in the presence of Verapamil indicating that the migratory effect of HEMO-IONIC was dependent on the release of its calcium ions.

3.9. Activation of the ERK signaling pathway in ECFCs by HEMO-IONIC

Activation of the signaling pathway involving phospho-ERK1/2 has been shown to induce endothelial cell proliferation, migration and angiogenesis [67,68]. Western blotting demonstrated that incubation of ECFCs with HEMO-IONIC CM induced reproducible transient expression of pERK1/2 (Fig. 4E).

3.10. In vivo effect of the hemostatic agents on tissue repair

The effect of the three hemostatic agents on tissue repair and formation of granulation tissue was assessed using a skin excision model in mice and compared to that of gauze. The numbers of macrophages, fibroblasts and blood vessels present in healing tissue at day 7 were quantified after contact with the four products (gauze, Surgicel, TachoSil, HEMO-IONIC).

3.10.1. Effect of hemostatic agents on macrophage numbers

The mean fluorescence intensities for the pan-macrophage marker (F4/80 receptor) were similar following application of Surgicel, TachoSil, and gauze (Fig. 5A): the number of infiltrated macrophages in the lesion was unchanged. With HEMO-IONIC, the fluorescence intensity was significantly increased relative to the other samples, by 72% *vs* gauze, 73% *vs* Surgicel, and 76% *vs* TachoSil ($p < 0.05$). Thus, of the three hemostatic agents tested, only HEMO-IONIC significantly increased the numbers of macrophages present within the healing tissue. Using specific markers for pro-inflammatory type 1 (CD80) and pro-healing type 2 (CD206) macrophages, an equivalent proportion of $CD80^+$ and $CD206^+$ macrophages was observed in the lesions with Gauze, Surgicel and TachoSil (Fig. S2). With HEMO-IONIC, a majority of the macrophages observed in the wound were $CD206^+$ macrophages. At day 14, the increase in macrophage number was no longer observed (data not shown), further indicating that application of HEMO-IONIC to the lesions does not exacerbate inflammation.

3.10.2. Effect of hemostatic agents on fibroblast numbers

The mean fluorescence intensities for the fibroblast marker Vimentin following application of Surgicel and TachoSil were very variable and were not significantly different from those recorded with gauze (Fig. 5B). In contrast, HEMO-IONIC significantly increased the fluorescence intensity for fibroblasts, by 45% vs gauze ($p < 0.01$). As for the macrophage numbers, only HEMO-IONIC significantly increased the numbers of fibroblasts within the lesion.

3.10.3. Effect of hemostatic agents on angiogenesis

After application of Surgicel and TachoSil, the number of blood vessels detected in tissue sections was similar to that recorded with gauze ($n_{blood\ vessels\ Surgicel} = 209$ and $n_{blood\ vessels\ TachoSil} = 269$ vs $n_{blood\ vessels\ gauze} = 251$ - Fig. 5C). However, in contrast with gauze, 89% of the vessels on the sections analyzed were distant from the site of application of the two hemostatic agents. With HEMO-IONIC, the number of blood vessels was strongly and significantly increased relative to gauze, Surgicel and TachoSil ($n_{blood\ vessels\ HEMO\text{-}IONIC} = 482$, $p < 0.001$). This increased number of blood vessels was transient and was no longer detected on day 14 after injury (data not shown), indicating that angiogenesis remained under control. In addition, blood vessels were observed throughout the lesion. These results demonstrate that only HEMO-IONIC promotes angiogenesis.

3.10.4. Effect of hemostatic agents on keratinocytes

The mean fluorescence intensities for the proliferation marker Ki67 measured in the epithelium following application of Surgicel and TachoSil were not significantly different from the gauze condition (Surgicel = 12.7; TachoSil = 8.2; gauze = 11.5; Fig. 5D). In contrast, HEMO-IONIC significantly increased keratinocyte proliferation vs gauze (HEMO-IONIC = 16.8; $p < 0.05$). These results demonstrate that HEMO-IONIC promotes epithelialization.

In conclusion, the results from tissue repair assays for macrophages, fibroblasts, blood vessels, and keratinocytes demonstrate that only HEMO-IONIC promotes the formation of granulation tissue and epithelialization.

3.11. Effect of the hemostatic agents on maturation of the extracellular matrix in scar tissue

To complete the *in vivo* analysis, maturation of the extracellular matrix was assessed in the skin excision repair model after 2 months, by analyzing collagen remodeling, as reflected by the collagen I/III ratio. In the presence of Surgicel, the collagen I/III ratio was similar to that recorded with gauze (Surgicel = 1.48 vs gauze = 1.45). In the presence of TachoSil, the ratio was decreased relative to gauze (1.30). Application of HEMO-IONIC increased the amount of collagen I without altering the amount of collagen III, resulting in a significant increase in the collagen I/III ratio relative to that recorded with gauze (1.63; $p < 0.0001$), and with Surgicel and TachoSil ($p < 0.001$) (Fig. 6). Thus, only HEMO-IONIC accelerates maturation of the extracellular matrix in scar tissue.

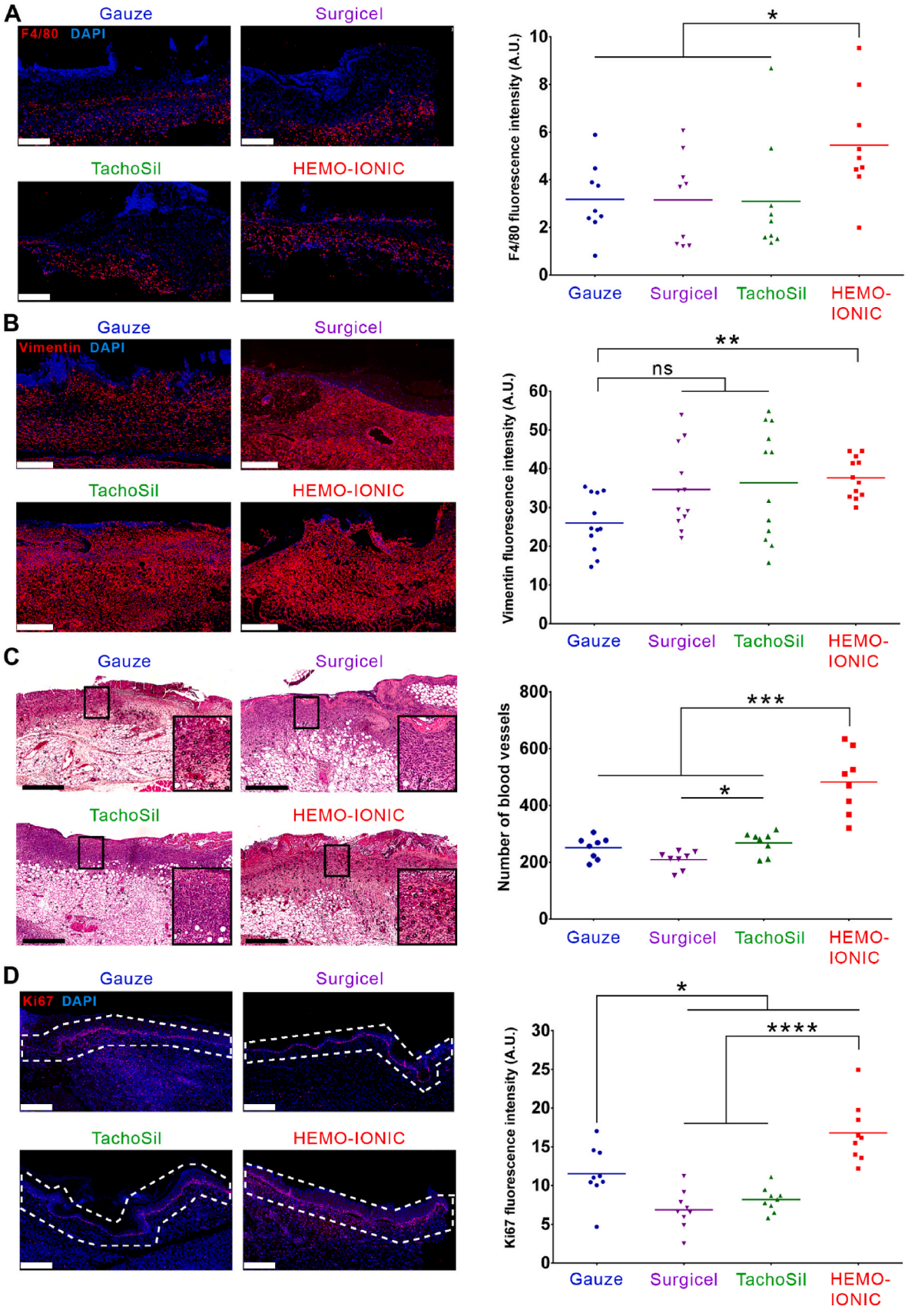

(caption on next page)

Fig. 5. Only HEMO-IONIC increases the numbers of macrophages, fibroblasts, blood vessels and keratinocytes in healing skin lesions
(**A-C**) The numbers of macrophages, fibroblasts and blood vessels were determined at D7 on sections prepared from lesions treated with gauze or the three hemostatic agents. (**A**) Representative immunofluorescence images from sections labelled with a macrophage marker (F4/80, red) and graph showing mean fluorescence intensities detected in the lesion (n = 9, Mann-Whitney test, *p < 0.05). Nuclei labelled with Hoechst (blue). (**B**) Representative immunofluorescence images from sections labelled with a fibroblast marker (vimentin, red) and graph showing mean fluorescence intensities detected in the lesion (n = 12, Mann-Whitney test, **p < 0.01). Nuclei labelled with Hoechst (blue). (**C**) Representative images of HES-stained sections (blood vessels are marked with the symbol ***O***; insets are enlarged 2.5X) and graph showing the number of blood vessels present (n = 8, Mann-Whitney test, *p < 0.05, ***p < 0.001). (**D**) Keratinocyte proliferation was assessed at D14 on sections prepared from lesions treated with gauze or the three hemostatic agents. Representative immunofluorescence images labelled with a proliferation marker (Ki67, red) and graph showing mean fluorescence intensities detected in the epithelium (n = 9, Mann-Whitney test, *p < 0.05, ****p < 0.0001). Nuclei labelled with Hoechst (blue). Scale bars = 250 μm.

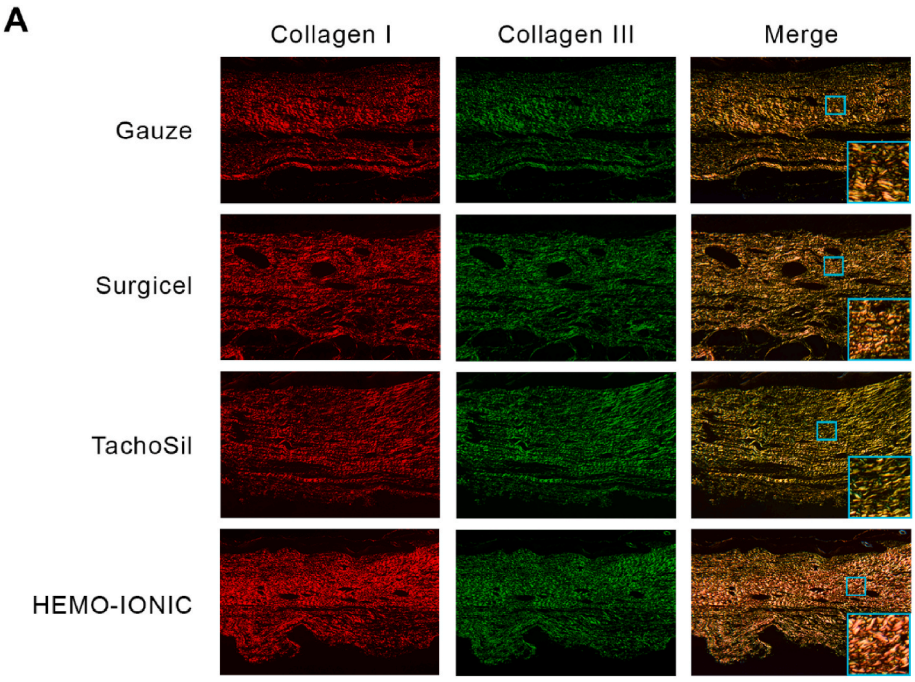

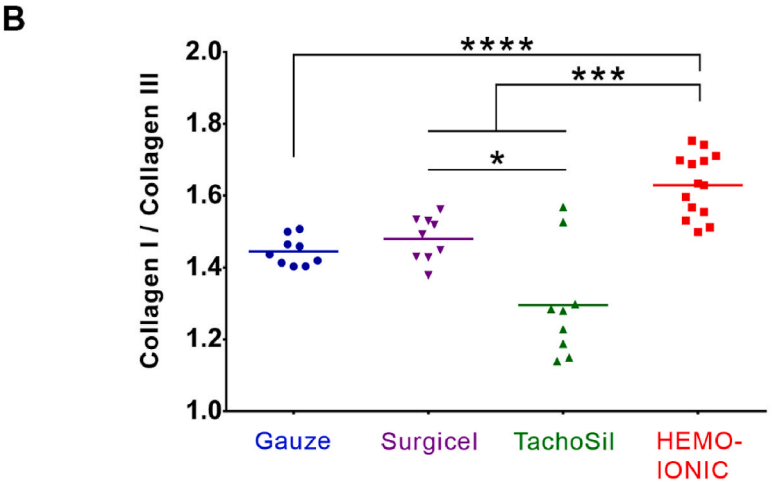

Fig. 6. Only HEMO-IONIC increases maturation of the extracellular matrix
(**A**) Representative images of sections prepared from lesions 2 months after treatment with gauze or the three hemostatic agents. Sections were stained with picrosirius red (Merge: collagen I, red and collagen III, green). (**B**) Graph showing collagen I/III ratios to assess maturation of the extracellular matrix (n = 9–14, Mann-Whitney test, *p < 0.05; ***p < 0.001; ****p < 0.0001).

4. Discussion

The aim of this study was to compare the effects on tissue repair of a new non-absorbable hemostatic agent, HEMO-IONIC (Zn^{2+}-enriched Ca^{2+} alginate), to the widely used absorbable surgical hemostatic agents Surgicel (oxidized regenerated cellulose) and TachoSil (collagen matrix soaked with fibrinogen and thrombin). HEMO-IONIC is a healing-promoting hemostatic agent which, upon contact with blood, induces formation of a stable clot through the release of calcium and zinc ions. As the ions are released, HEMO-IONIC can be removed from the surgical site without causing renewed bleeding, removal also helps avoid any reaction to the presence of a foreign body in the tissue as it heals. Surgicel and TachoSil act on hemostasis by mechanical action, by creating frameworks for platelet aggregation. They must remain *in situ* after hemostasis is established, and thus may trigger a foreign body reaction as described in the literature [13,17,18]. The effects on tissue repair of these two hemostatic agents left *in situ* have been little studied. Here, we examined the hypothesis that, relative to Surgicel and TachoSil,

HEMO-IONIC would allow better tissue repair, and consequently accelerated recovery for the patient, not only due to the absence of foreign bodies, but also thanks to its healing-promoting effect.

After comparing the hemostatic efficacy of the three products *in vitro* and *in vivo*, we assessed their *in vitro* effects on the activation of endothelial cells (ECFCs) *in vitro*. These cells were chosen for their involvement in all the phases of tissue repair. Finally, the *in vivo* effect of the three hemostatics on tissue repair in a murine skin excision model was studied.

4.1. Hemostasis

As a preliminary study, we validated the hemostatic efficacy of HEMO-IONIC in comparison with the absorbable hemostatic agents Surgicel and TachoSil. The *in vitro* results on blood coagulation demonstrated that HEMO-IONIC performed significantly better than Surgicel and similarly to TachoSil (Fig. S1A). *In vivo*, in a pig liver lesion model, hemostasis was reached with HEMO-IONIC in less than 5 min similar to Surgicel (Fig. S1B). This result demonstrates the high efficacy of HEMO-IONIC, as the experimental set-up was designed to test hemostatic agents used in first intention, in a context of extensive hemorrhage, even though this is not their indication. Rather, hemostatic agents are indicated for use secondary to conventional techniques (electro-coagulation for example). Based on the *in vitro* and *in vivo* results obtained, HEMO-IONIC appears to be as effective as the hemostatic agents Surgicel and TachoSil.

After hemostasis was obtained on mouse liver lesions, it was possible to remove HEMO-IONIC without adhesion and renewed bleeding. In contrast, both Surgicel and Tachosil adhered to the tissue, making them difficult to remove, and their removal led to renewed bleeding (Fig. 1B and supplementary movies M1-M4). Numerous clinical studies have shown that calcium alginate promotes hemostasis and is compatible with non-traumatic removal from tissues [22–24]. Our results are in line with those of a published study demonstrating that calcium alginate leads to better platelet aggregation and improved clot stability compared to oxidized regenerated cellulose or collagen hemostatic agents [69]. The authors of this previous study also confirmed that Zn^{2+}-supplementation of calcium alginate increased platelet aggregation and thrombin formation.

The hemostatic performance of HEMO-IONIC can be explained by its bioactivity: upon contact with blood, HEMO-IONIC exchanges its calcium and zinc ions for circulating Na^{+}. Ca^{2+}, in its role as coagulation factor IV, is required for all of the enzymatic reactions leading to the generation of fibrin and clot formation [70,71]. In parallel, Zn^{2+} increases platelet aggregation and contributes, as an enzymatic cofactor, to the progress and regulation of coagulation [34]. In line with these roles, our results show that Zn^{2+} adjunction improves plasma coagulation compared to pure Ca^{2+} alginate (Fig. S1E). We also demonstrated, *in vitro* on ECFCs, that in the presence of HEMO-IONIC, the secretion of endothelin-1 (vasoconstrictor) and the expression of tissue factor (glycoprotein activating the coagulation cascade) were significantly increased compared to the control condition (Figs. S1C and S1D). This result demonstrates that HEMO-IONIC can further act on hemostasis *in vivo* by activating the vascular stage.

4.2. Endothelial cell activation

The effects of the three hemostatic agents on endothelial cells and angiogenesis were assessed *in vitro* by exposing ECFCs to their CM, in accordance with ISO 10993–12:2012 [72] and monitoring cell survival, activity and migration.

Results from these assays demonstrated that the Surgicel CM (acidic pH of 5) induced the death of 92% of ECFCs, compared to just 4% death induced by media conditioned with TachoSil and HEMO-IONIC. To allow us to perform experiments on the endothelial functions of ECFCs, the Surgicel CM was neutralized to pH = 7. Even after neutralization, Surgicel CM significantly slowed ECFC proliferation, reduced metabolic activity, and inhibited migration in response to VEGF. These results corroborate those of studies demonstrating that the acidic pH of regenerated oxidized cellulose is only one reason for inhibited proliferation and cellular migration, suggesting that this hemostatic agent releases other substances that have a toxic effect [73,74]. The acidic pH and strong toxicity observed with Surgicel could explain the numerous adverse events reported following its clinical application (necrosis, abscess, etc.) [10,11,13,15,16,75]. *In vitro*, TachoSil preserved endothelial cell viability and proliferation. However, it significantly reduced metabolic activity and inhibited migration. The strong negative impact of TachoSil on endothelial cell migration in the presence or absence of VEGF could be explained by the fibrinogen-E fragment, a product of fibrinogen – which is a component of TachoSil – degradation. According to the literature, this fragment exerts a powerful antiangiogenic effect (*in vitro* and *in vivo*) and inhibits endothelial cell migration [76,77]. In contrast, HEMO-IONIC preserved viability, proliferation and metabolic activity in ECFCs, it also induced a strong increase in migration even in the absence of VEGF, demonstrating its chemo-attractant effect. HEMO-IONIC-induced migration was significantly decreased in the presence of Verapamil, a specific calcium antagonist, confirming the involvement of calcium ions released by HEMO-IONIC in its chemo-attractant effect on ECFCs. HEMO-IONIC also activated the ERK1/2 pathway, which is known to induce endothelial cell proliferation, migration and angiogenesis [67,68], by inducing its phosphorylation.

4.3. Tissue repair

The *in vitro* results obtained with ECFCs were confirmed by the results of *in vivo* studies on skin excision in mice. Skin excision is considered a predictive model of clinical wound healing [78]. In this model, to remain consistent with their use in the clinic, Surgicel and TachoSil (absorbable) were left in contact with the excision until the neoformed tissue was sampled; HEMO-IONIC and the Control gauze (non-absorbable) were removed after 10 min' application.

Seven days after a 10-min application, relative to gauze, HEMO-IONIC was the only hemostatic agent which significantly increased the number of macrophages (with a majority of pro-healing $CD206^{+}$ macrophages) and fibroblasts present in the recovering tissue; it also increased the number of blood vessels (pro-angiogenic effect). Fourteen days after excision, only HEMO-IONIC significantly increased proliferation of keratinocytes.

During the proliferation phase, the formation of granulation tissue is characterized by both (1) migration and proliferation of fibroblasts that secrete the components necessary for the production and maturation of the new matrix and (2) the formation of new blood vessels that supply the forming tissue with oxygen and nutrients. As it is removed, HEMO-IONIC does not interfere with the migration and proliferation of fibroblasts, endothelial cells and keratinocytes (no physical barrier left). This could partly explain the increased number of fibroblasts and blood vessels and the keratinocyte proliferation observed in our mouse skin excision model. Moreover, our *in vitro* data reporting increased cell migration demonstrate that HEMO-IONIC can directly activate endothelial cells. In addition, unlike absorbable hemostatic agents such as Surgicel and TachoSil, removal of HEMO-IONIC eliminates the risk of foreign body reactions that can hinder tissue repair [17,18].

After seven days of *in situ* contact with Surgicel and TachoSil, the numbers of macrophages, fibroblasts and blood vessels were similar to those present in the gauze sample. However, in the Surgicel and TachoSil conditions, and in contrast with gauze, the blood vessels tended to remain at a distance from the hemostatic agents and did not completely colonize the neoformed tissue. This result confirms the toxic effects of Surgicel and the inhibition of migration of endothelial cells observed with TachoSil *in vitro*. The negative effects obtained with these hemostatic agents, associated with the fact that they remain in place (reaction to foreign bodies and physical barrier to cell proliferation and

migration) may hinder tissue repair in the resected organ, and consequently delay recovery for the patient.

Two months after excision, the lesions treated with all three hemostatic agents had completely healed over. However, remodeling of the extracellular matrix, quantified by the increase in the collagen I/III ratio, was only significantly accelerated compared to gauze in animals treated with HEMO-IONIC. Tissue maturation is characterized by the progressive replacement of the temporary extracellular matrix, mainly composed of fibrin and collagen III, by a definitive extracellular matrix, mainly composed of collagen I. The higher numbers of fibroblasts within the tissue reported in this work in the early stages of tissue repair might have boosted the production of Collagen I and Zn-dependent MMPs, and thus led to accelerated matrix maturation.

The breakdown of tissue repair into three main consecutive phases (inflammation, proliferation and maturation) is artificial. In reality, these phases partially overlap and interact with each other over time [50]. We hypothesize that the release of calcium and zinc ions from HEMO-IONIC into the wounded area boosts the activation of key tissue repair cells (macrophages, fibroblasts, endothelial cells …) at the beginning of the process, setting the stage for a positive chain reaction that continues throughout subsequent tissue repair phases.

Calcium ions are central regulators of tissue repair [28,79]. The Ca^{2+} signal is a universal and effective cell activation signal, which results from an increase in the cytoplasmic Ca^{2+} concentration from less than 100 nM at rest to 500–1000 nM upon activation [66,80]. The Ca^{2+} signal regulates the proliferation and migration of endothelial cells [81–83], as well as activating macrophages [84–86], fibroblasts [87,88], and keratinocytes [89]. Upon contact with HEMO-IONIC, the cytoplasmic Ca^{2+} concentration in ECFCs increased to 860 nM, demonstrating that HEMO-IONIC releases an optimal level of calcium ions to induce cellular activation.

The zinc ions released by HEMO-IONIC also stimulate endothelial cells (proliferation, migration) and promote angiogenesis [90]. In addition, Zn^{2+} contributes to all of the phases of repair through its role as a cofactor to numerous proteins and enzymes [91–93]: regulation of the inflammatory phase [94,95], cellular activation and proliferation [92,96].

Finally, the two ions promote remodeling of the extracellular matrix: the calcium ions via activation of fibroblasts, and the zinc ions through their role as cofactors of MMPs [97].

5. Conclusions

This study analyzed the effects of surgical hemostatic agents *in vitro* on endothelial cells and *in vivo* on tissue repair. The results show that with a hemostatic efficacy comparable to Surgicel and TachoSil, HEMO-IONIC provides two advantages: it is removed from the surgical site (no risk of subsequent reaction to a foreign body), and it promotes wound healing (including angiogenesis) after only 10 min' application. Given that the composition of alginate dressings differs strongly [35,98] and that the levels of calcium ions released by an alginate depend on numerous physicochemical parameters (Na^+ alginate/Ca^{2+} alginate ratio; mannuronic acid/guluronic acid ratio, etc.), the results of this study cannot be extrapolated to other alginates [99,100]. The cellular toxicity observed with Surgicel and TachoSil is a reminder of the importance of being fully aware of the effects of medical devices left *in situ* to avoid delaying tissue repair. The results of this study indicate that HEMO-IONIC is a very promising surgical hemostatic agent in terms of efficacy, safety and potential benefit for the patient. Moreover, the estimated cost of HEMO-IONIC (10 × 20 cm) compares very favorably with Surgicel (2.5 × 7.5 cm) and TachoSil (9.5 × 4.8 cm), based on established list-prices [101]. The results of this study provide the elements required to support a comparative clinical study of the three hemostatic agents, to measure the speed and quality of tissue repair.

CRediT authorship contribution statement

Anne-Charlotte Ponsen: Conceptualization, Methodology, Investigation, Formal analysis, Writing – original draft, Writing – review & editing. **Richard Proust:** Methodology, Validation, Formal analysis, Investigation, Writing – original draft, Writing – review & editing. **Sabrina Soave:** Investigation, Writing – review & editing. **Françoise Mercier-Nomé:** Investigation, Resources, Writing – review & editing. **Isabelle Garcin:** Methodology, Validation, Writing – review & editing. **Laurent Combettes:** Methodology, Validation, Resources, Writing – review & editing. **Jean-Jacques Lataillade:** Conceptualization, Validation, Resources, Supervision, Writing – review & editing. **Georges Uzan:** Conceptualization, Validation, Resources, Supervision, Funding acquisition, Writing – review & editing.

Declaration of competing interest

Anne-Charlotte Ponsen was employed at BROTHIER during her PhD. The other authors have not indicated any potential conflict of interest.

Acknowledgements

We are very grateful to Dr. Florence Armstrong for her scientific advice and for participating in supervision of A-C.P.'s PhD research. We also express our gratitude to Dr. Céline Revenu for her help in writing the article. We thank Dr. Claude Boucheix for his scientific advice and for proofreading of the paper. We are grateful to the UMS-44 (ex UMS-33) for providing access to its many platforms, and especially to Denis Clay, who runs the Cytometry platform, as well as the whole team at the animal house. We warmly thank Aurore Devocelle, Antonietta Messina, Nassima Benzoubir, and Marwa Hussein for their help with experiments performed to help answer the reviewers' questions. Finally, we would like to thank the Direction Générale de l'Armement (DGA) which partially financed A-C.P.'s PhD in the context of a CIFRE-Défense thesis (n° 10/2014/DGA), in particular Dr. Emmanuelle Guillot-Combe, who is responsible for the follow-up of the PhD students.

Appendix A. Supplementary data

Supplementary data to this article can be found online at https://doi.org/10.1016/j.bioactmat.2022.01.049.

References

[1] S. Nazeer, M.I. Shafi, Principles of surgical technique, in: E.J. Bieber, I. R. Horowitz, J.S. Sanfilippo, M.I. Shafi (Eds.), Clinical Gynecology, 2 ed., Cambridge University Press, Cambridge, 2015, pp. 297–306.
[2] M.D. Palm, J.S. Altman, Topical hemostatic agents: a review, Dermatol. Surg. 34 (2008) 431–445.
[3] M. Hamon, M. Dupres, S. Wisniewski, Produits pharmaceutiques à visée hémostatique : physiopathologie, propriétés et utilisation, Le pharmacien hospitalier et clinicien 51 (2016) 3–18.
[4] H. Seyednejad, M. Imani, T. Jamieson, A.M. Seifalian, Topical haemostatic agents, Br. J. Surg. 95 (2008) 1197–1225.
[5] A. Frilling, G.A. Stavrou, H.J. Mischinger, B. de Hemptinne, M. Rokkjaer, J. Klempnauer, et al., Effectiveness of a new carrier-bound fibrin sealant versus argon beamer as haemostatic agent during liver resection: a randomised prospective trial, Langenbeck's Arch. Surg. 390 (2005) 114–120.
[6] Y. Genyk, T. Kato, J.J. Pomposelli, J.K. Wright Jr., L.S. Sher, V. Tetens, et al., Fibrin sealant patch (TachoSil) vs oxidized regenerated cellulose patch (Surgicel original) for the secondary treatment of local bleeding in patients undergoing hepatic resection: a randomized controlled trial, J. Am. Coll. Surg. 222 (2016) 261–268.
[7] J.B. Hanks, H.K. Kjaergard, D.A. Hollingsbee, A comparison of the haemostatic effect of Vivostat patient-derived fibrin sealant with oxidised cellulose (Surgicel) in multiple surgical procedures, Eur. Surg. Res. 35 (2003) 439–444.
[8] A. Rickenbacher, S. Breitenstein, M. Lesurtel, A. Frilling, Efficacy of TachoSil a fibrin-based haemostat in different fields of surgery–a systematic review, Expet Opin. Biol. Ther. 9 (2009) 897–907.
[9] F. Kakaei, M.S. Seyyed Sadeghi, B. Sanei, S. Hashemzadeh, A. Habibzadeh, A randomized clinical trial comparing the effect of different haemostatic agents

for haemostasis of the liver after hepatic resection, HPB Surg. : World J. Hepatic. Pancreat.Biliary.Surg. (2013) 5.
[10] R. Abs, [Cutaneous necrosis in a clinical case of one face lift after the use of Surgicel], Ann. Chir. Plast. Esthet. 49 (2004) 43–46.
[11] M.M. Agarwal, A.K. Mandal, S. Agarwal, A. Lal, M. Prakash, R. Mavuduru, et al., Surgicel granuloma: unusual cause of "Recurrent" mass lesion after laparoscopic nephron-sparing surgery for renal cell carcinoma, Urology 76 (2010) 334–335.
[12] L. Fischer, C.M. Seiler, C.E. Broelsch, B. de Hemptinne, J. Klempnauer, H. J. Mischinger, et al., Hemostatic efficacy of TachoSil in liver resection compared with argon beam coagulator treatment: an open, randomized, prospective, multicenter, parallel-group trial, Surgery 149 (2011) 48–55.
[13] M.F. Ibrahim, C. Aps, C.P. Young, A foreign body reaction to Surgicel mimicking an abscess following cardiac surgery, Eur. J. Cardio. Thorac. Surg. 22 (2002) 489–490, author reply 90.
[14] S. Kawasaki, H. Origasa, V. Tetens, M. Kobayashi, Comparison of TachoSil and TachoComb in patients undergoing liver resection-a randomized, double-blind, non-inferiority trial, Langenbeck's Arch. Surg. 402 (2017) 591–598.
[15] M. Partheni, C. Kalogheropoulou, N. Karageorgos, V. Panagiotopoulos, S. Voulgaris, F. Tzortzidis, Radiculopathy after lumbar discectomy due to intraspinal retained Surgicel: clinical and magnetic resonance imaging evaluation, Spine J. 6 (2006) 455–458.
[16] A. Teis, M.L. Camara, E. Ferrer, B. Romero-Ferrer, Critical stenosis of pulmonary homograft induced by Surgicel in Ross procedure, Asian Cardiovasc. Thorac. Ann. 18 (2010) 382–383.
[17] Y. Tomizawa, Clinical benefits and risk analysis of topical hemostats: a review, J. Artif. Organs 8 (2005) 137–142.
[18] H.S. Yoon, Y.C. Na, K.H. Choi, W.H. Huh, J.M. Kim, Wound healing effect of regenerated oxidized cellulose versus fibrin sealant patch: an in vivo study, Archives of craniofacial surgery 20 (2019) 289–296.
[19] G. van Der Bie, T. Scheffers, C. van Tellingen, The Healing Process - Organ of Repair, Driebergen: Louis Bolk Instituut, 2008.
[20] K.S. Vyas, S.P. Saha, Comparison of hemostatic agents used in vascular surgery, Expet Opin. Biol. Ther. 13 (2013) 1663–1672.
[21] O. Ljungqvist, M. Scott, K.C. Fearon, Enhanced recovery after surgery: a review, JAMA surgery 152 (2017) 292–298.
[22] M. Pannier, V. Martinot, J.C. Castède, J. Guitard, M. Robert, A. Le Touze, et al., Evaluation de l'efficacité et de la tolérance d'Algostéril (compresse d'alginate de calcium) versus Jelonet (gaze paraffinée) dans le traitement du site donneur de greffe dermo-épidermique du cuir chevelu. Résultats d'un essai pédiatrique, Ann. Chir. Plast. Esthet. 47 (2002) 285–290.
[23] S.D. Blair, P. Jarvis, M. Salmon, C. McCollum, Clinical trial of calcium alginate haemostatic swabs, Br. J. Surg. 77 (1990) 568–570.
[24] M.S. Davies, M.C. Flannery, C.N. McCollum, Calcium alginate as haemostatic swabs in hip fracture surgery, J. R. Coll. Surg. Edinb. 42 (1997) 31–32.
[25] S. Thomas, Alginate dressings in surgery and wound management: Part 2, J. Wound Care 9 (2000) 115–119.
[26] PS C, P W, Alginates: wound dressings. Encyclopedia of Biomedical Polymers and Polymeric Biomaterials first ed., vol. 11, CRC Press, Boca Raton, 2015, p. 13p.
[27] H.C. Segal, B.J. Hunt, K. Gilding, The effects of alginate and non-alginate wound dressings on blood coagulation and platelet activation, J. Biomater. Appl. 12 (1998) 249–257.
[28] A.B. Lansdown, Calcium: a potential central regulator in wound healing in the skin (version originale), Wound Repair Regen. 10 (2002) 271–285.
[29] T.J. McNulty, C.W. Taylor, Extracellular heavy-metal ions stimulate Ca2+ mobilization in hepatocytes, Biochem. J. 339 (Pt 3) (1999) 555–561.
[30] M. Hershfinkel, A. Moran, N. Grossman, I. Sekler, A zinc-sensing receptor triggers the release of intracellular Ca2+ and regulates ion transport, Proc. Natl. Acad. Sci. U. S. A 98 (2001) 11749–11754.
[31] E.M. Schwiebert, L. Liang, N.-L. Cheng, C.R. Williams, D. Olteanu, E.A. Welty, et al., Extracellular zinc and ATP-gated P2X receptor calcium entry channels: new zinc receptors as physiological sensors and therapeutic targets, Purinergic Signal. 1 (2005) 299–310.
[32] A.B. Lansdown, U. Mirastschijski, N. Stubbs, E. Scanlon, M.S. Agren, Zinc in wound healing: theoretical, experimental, and clinical aspects, Wound Repair Regen. 15 (2007) 2–16.
[33] Kietzmann, Improvement and retardation of wound healing: effects of pharmacological agents in laboratory animal studies, Vet. Dermatol. 10 (1999) 83–88.
[34] T.T. Vu, J.C. Fredenburgh, J.I. Weitz, Zinc: an important cofactor in haemostasis and thrombosis, Thromb. Haemostasis 109 (2013) 421–430.
[35] Y. Qin, The gel swelling properties of alginate fibers and their applications in wound management, Polym. Adv. Technol. 19 (2008) 6–14.
[36] L. Maggiori, E. Rullier, C. Meyer, G. Portier, J.L. Faucheron, Y. Panis, Randomized controlled trial of pelvic calcium alginate following rectal cancer surgery, Br. J. Surg. 97 (2010) 479–484.
[37] S.A. Eming, B. Brachvogel, T. Odorisio, M. Koch, Regulation of angiogenesis: wound healing as a model, Prog. Histochem. Cytochem. 42 (2007) 115–170.
[38] J. Hu, K. Srivastava, M. Wieland, A. Runge, C. Mogler, E. Besemfelder, et al., Endothelial cell-derived angiopoietin-2 controls liver regeneration as a spatiotemporal Rheostat, Science 343 (2014) 416–419.
[39] M.A. Ross, C.M. Sander, T.B. Kleeb, S.C. Watkins, D.B. Stolz, Spatiotemporal expression of angiogenesis growth factor receptors during the revascularization of regenerating rat liver, Hepatology 34 (2001) 1135–1148.
[40] B.-S. Ding, D.J. Nolan, J.M. Butler, D. James, A.O. Babazadeh, Z. Rosenwaks, et al., Inductive angiocrine signals from sinusoidal endothelium are required for liver regeneration, Nature 468 (2010) 310–315.
[41] B.-S. Ding, J. Nolan Daniel, P. Guo, O. Babazadeh Alexander, Z. Cao, Z. Rosenwaks, et al., Endothelial-derived angiocrine signals induce and sustain regenerative lung alveolarization, Cell 147 (2011) 539–553.
[42] N. Woik, J. Kroll, Regulation of lung development and regeneration by the vascular system, Cell. Mol. Life Sci. 72 (2015) 2709–2718.
[43] O.L. Kathy, VEGF-A: the inductive angiogenic factor for development, regeneration and function of pancreatic beta cells, Curr. Stem Cell Res. Ther. 9 (2014) 396–400.
[44] S.D. Rivas-Carrillo, J. Kanamune, Y. Iwanaga, S. Uemoto, A. Daneri-Navarro, J. D. Rivas-Carrillo, Endothelial cells promote pancreatic stem cell activation during islet regeneration in mice, Transplant. Proc. 43 (2011) 3209–3211.
[45] V. Talman, R. Kivelä, Cardiomyocyte—endothelial cell interactions in cardiac remodeling and regeneration, Front. Cardiovasc. Med. 5 (2018).
[46] D.A. Narmoneva, R. Vukmirovic, M.E. Davis, R.D. Kamm, R.T. Lee, Endothelial cells promote cardiac myocyte survival and spatial Reorganization, Circulation 110 (2004) 962–968.
[47] S.A. Eming, T. Krieg, J.M. Davidson, Inflammation in wound repair: molecular and cellular mechanisms, J. Invest. Dermatol. 127 (2007) 514–525.
[48] J.S. Pober, W.C. Sessa, Evolving functions of endothelial cells in inflammation, Nat. Rev. Immunol. 7 (2007) 803–815.
[49] G. Broughton 2nd, J.E. Janis, C.E. Attinger, Wound healing: an overview, Plast. Reconstr. Surg. 117 (2006) 1e. S-32e-S.
[50] J.M. Reinke, H. Sorg, Wound repair and regeneration, Eur. Surg. Res. 49 (2012) 35–43.
[51] P. Bainbridge, Wound healing and the role of fibroblasts, J. Wound Care 22 (407–8) (2013) 10–12.
[52] N.S. Greaves, K.J. Ashcroft, M. Baguneid, A. Bayat, Current understanding of molecular and cellular mechanisms in fibroplasia and angiogenesis during acute wound healing, J. Dermatol. Sci. 72 (2013) 206–217.
[53] J. Pizzicannella, F. Diomede, I. Merciaro, S. Caputi, A. Tartaro, S. Guarnieri, et al., Endothelial committed oral stem cells as modelling in the relationship between periodontal and cardiovascular disease, J. Cell. Physiol. 233 (2018) 6734–6747.
[54] M.C. Yoder, Differentiation of pluripotent stem cells into endothelial cells, Curr. Opin. Hematol. 22 (2015) 252–257.
[55] V. Vanneaux, F. El-Ayoubi, C. Delmau, C. Driancourt, S. Lecourt, A. Grelier, et al., In vitro and in vivo analysis of endothelial progenitor cells from cryopreserved umbilical cord blood: are we ready for clinical application? Cell Transplant. 19 (2010) 1143–1155.
[56] P. Au, L.M. Daheron, D.G. Duda, K.S. Cohen, J.A. Tyrrell, R.M. Lanning, et al., Differential in vivo potential of endothelial progenitor cells from human umbilical cord blood and adult peripheral blood to form functional long-lasting vessels, Blood 111 (2008) 1302–1305.
[57] H. Bompais, J. Chagraoui, X. Canron, M. Crisan, X.H. Liu, A. Anjo, et al., Human endothelial cells derived from circulating progenitors display specific functional properties compared with mature vessel wall endothelial cells, Blood 103 (2004) 2577–2584.
[58] D.A. Ingram, L.E. Mead, H. Tanaka, V. Meade, A. Fenoglio, K. Mortell, et al., Identification of a novel hierarchy of endothelial progenitor cells using human peripheral and umbilical cord blood, Blood 104 (2004) 2752–2760.
[59] V. Jones, J.E. Grey, K.G. Harding, Wound dressings, Bmj 332 (2006) 777–780.
[60] F. Chevalier, M. Lavergne, E. Negroni, S. Ferratge, G. Carpentier, M. Gilbert-Sirieix, et al., Glycosaminoglycan mimetic improves enrichment and cell functions of human endothelial progenitor cell colonies, Stem Cell Res. 12 (2014) 703–715.
[61] G. Grynkiewicz, M. Poenie, R.Y. Tsien, A new generation of Ca2+ indicators with greatly improved fluorescence properties, J. Biol. Chem. 260 (1985) 3440–3450.
[62] W.J. Lindblad, Considerations for selecting the correct animal model for dermal wound-healing studies, J. Biomater. Sci. Polym. Ed. 19 (2008) 1087–1096.
[63] L. Chen, R. Mirza, Y. Kwon, L.A. DiPietro, T.J. Koh, The murine excisional wound model: contraction revisited, Wound Repair Regen. 23 (2015) 874–877.
[64] H.D. Zomer, A.G. Trentin, Skin wound healing in humans and mice: challenges in translational research, J. Dermatol. Sci. 90 (2018) 3–12.
[65] J. Li, J. Chen, R. Kirsner, Pathophysiology of acute wound healing, Clin. Dermatol. 25 (2007) 9–18.
[66] M.J. Berridge, P. Lipp, M.D. Bootman, The versatility and universality of calcium signalling, Nat. Rev. Mol. Cell Biol. 1 (2000) 11–21.
[67] J. Krupinski, M. Abudawood, S. Matou-Nasri, R. Al-Baradie, E.B. Petcu, C. Justicia, et al., Citicoline induces angiogenesis improving survival of vascular/human brain microvessel endothelial cells through pathways involving ERK1/2 and insulin receptor substrate-1, Vasc. Cell 4 (2012) 20.
[68] M. Slevin, P. Kumar, J. Gaffney, S. Kumar, J. Krupinski, Can angiogenesis be exploited to improve stroke outcome? Mechanisms and therapeutic potential, Clin Sci (Lond). 111 (2006) 171–183.
[69] S.D. Blair, C.M. Backhouse, R. Harper, J. Matthews, C.N. McCollum, Comparison of absorbable materials for surgical haemostasis, Br. J. Surg. 75 (1988) 969–971.
[70] H.M.H. Spronk, J.W.P. Govers-Riemslag, H. ten Cate, The blood coagulation system as a molecular machine, Bioessays 25 (2003) 1220–1228.
[71] J.C. Giddings, The Role of Calcium in Biological Systems: Calcium in Blood Coagulation and Hemostasis, CRC Press I, 1982.
[72] C. Pellevoisin, F. Cottrez, J. Johansson, E. Pedersen, K. Coleman, H. Groux, Pre-validation of SENS-IS assay for in vitro skin sensitization of medical devices, Toxicol. Vitro : Int. J.Publ. Assoc.BIBRA 71 (2021) 105068.
[73] B. Hexig, R. Nakaoka, T. Tsuchiya, Safety evaluation of surgical materials by cytotoxicity testing, J. Artif. Organs 11 (2008) 204–211.

[74] M.U. Wagenhäuser, J. Mulorz, W. Ibing, F. Simon, J.M. Spin, H. Schelzig, et al., Oxidized (non)-regenerated cellulose affects fundamental cellular processes of wound healing, Sci. Rep. 6 (2016) 32238.
[75] S.C. Buckley, J.C. Broome, A foreign body reaction to Surgicel(R) mimicking an abscess or tumour recurrence, Br. J. Neurosurg. 9 (1995) 561–563.
[76] C.A. Bootle-Wilbraham, S. Tazzyman, J.M. Marshall, C.E. Lewis, Fibrinogen E-fragment inhibits the migration and tubule formation of human dermal microvascular endothelial cells in Vitro</em&gt, Cancer Res. 60 (2000) 4719–4724.
[77] M.E. Daly, A. Makris, M. Reed, C.E. Lewis, Hemostatic regulators of tumor angiogenesis: a source of antiangiogenic agents for cancer treatment? JNCI: J. Natl. Cancer Inst. 95 (2003) 1660–1673.
[78] L. Dunn, H.C.G. Prosser, J.T.M. Tan, L.Z. Vanags, M.K.C. Ng, C.A. Bursill, Murine model of wound healing, JoVE (2013), e50265.
[79] S.J. Ghilardi, B.M. O'Reilly, A.E. Sgro, Intracellular signaling dynamics and their role in coordinating tissue repair, Wiley Interdiscip. Rev. Syst. Biol.Med. 12 (2020) e1479.
[80] D.E. Clapham, Calcium signaling, Cell 131 (2007) 1047–1058.
[81] F. Moccia, Calcium signaling in endothelial Colony forming cells in health and disease, Adv. Exp. Med. Biol. 1131 (2020) 1013–1030.
[82] F. Moccia, S. Negri, M. Shekha, P. Faris, G. Guerra, Endothelial Ca2+ signaling, angiogenesis and Vasculogenesis: just what it takes to make a blood vessel, Int. J. Mol. Sci. 20 (2019) 3962.
[83] F. Moccia, F. Lodola, S. Dragoni, E. Bonetti, C. Bottino, G. Guerra, et al., Ca^{2+} signalling in endothelial progenitor cells: a novel means to improve cell-based therapy and impair tumour Vascularisation, Curr. Vasc. Pharmacol. 12 (2014) 87–105.
[84] B.N. Desai, N. Leitinger, Purinergic and calcium signaling in macrophage function and plasticity, Front. Immunol. 5 (2014).
[85] S. Tedesco, V. Scattolini, M. Albiero, M. Bortolozzi, A. Avogaro, A. Cignarella, et al., Mitochondrial calcium uptake is instrumental to alternative macrophage polarization and phagocytic activity, Int. J. Mol. Sci. 20 (2019) 4966.
[86] S. Feske, H. Wulff, E.Y. Skolnik, Ion channels in innate and adaptive immunity, Annu. Rev. Immunol. 33 (2015) 291–353.
[87] C. Navarro-Requena, S. Pérez-Amodio, O. Castaño, E. Engel, Wound healing-promoting effects stimulated by extracellular calcium and calcium-releasing nanoparticles on dermal fibroblasts, Nanotechnology 29 (2018) 395102.
[88] L. Follonier Castella, G. Gabbiani, C.A. McCulloch, B. Hinz, Regulation of myofibroblast activities: calcium pulls some strings behind the scene, Exp. Cell Res. 316 (2010) 2390–2401.
[89] C.-L. Tu, A. Celli, T. Mauro, W. Chang, Calcium-Sensing receptor regulates epidermal intracellular Ca2+ signaling and Re-epithelialization after wounding, J. Invest. Dermatol. 139 (2019) 919–929.
[90] D. Zhu, Y. Su, Y. Zheng, B. Fu, L. Tang, Y.X. Qin, Zinc regulates vascular endothelial cell activity through zinc-sensing receptor ZnR/GPR39, Am. J. Physiol. Cell Physiol. 314 (2018). C404-c14.
[91] C.J. Frederickson, J.Y. Koh, A.I. Bush, The neurobiology of zinc in health and disease, Nat. Rev. Neurosci. 6 (2005) 449–462.
[92] R.S. MacDonald, The role of zinc in growth and cell proliferation, J. Nutr. 130 (2000), 1500S-8S.
[93] W. Maret, Zinc in cellular regulation: the nature and significance of "zinc signals, Int. J. Mol. Sci. 18 (2017).
[94] M. Sapkota, D.L. Knoell, Essential role of zinc and zinc transporters in myeloid cell function and host defense against infection, J. Immunol. Res. (2018) 4315140.
[95] H. Haase, L. Rink, Zinc signals and immune function, Biofactors 40 (2014) 27–40.
[96] M.N. Lo, L.J. Damon, J. Wei Tay, S. Jia, A.E. Palmer, Single cell analysis reveals multiple requirements for zinc in the mammalian cell cycle, Elife 9 (2020).
[97] P.-H. Lin, M. Sermersheim, H. Li, P.H.U. Lee, S.M. Steinberg, J. Ma, Zinc in wound healing modulation, Nutrients 10 (2018) 16.
[98] K. Varaprasad, T. Jayaramudu, V. Kanikireddy, C. Toro, E.R. Sadiku, Alginate-based composite materials for wound dressing application:A mini review, Carbohydr. Polym. 236 (2020) 116025.
[99] Y. Qin, The characterization of alginate wound dressings wih different fiber and textile structures, J. Appl. Polym. Sci. 100 (2006) 2516–2520.
[100] S. Thomas, Alginate dressings in surgery and wound management: Part 3, J. Wound Care 9 (2000) 163–166.
[101] D. Bresson, H. Barreteau, Place des agents hémostatiques locaux en neurochirurgie : chirurgie spinale et intracrânienne, Le Pharmacien hospitalier et Clinicien 51 (2016) 29–41.